

High-Density Helicon Plasma Thrusters Using Electrodeless Acceleration Schemes

By Daisuke KUWAHARA, Shunjiro SHINOHARA, Takamichi ISHII, Shuhei OTSUKA,
Toshiki NAKAGAWA, Kensuke KISHI, Marie SAKATA, Eiko TANAKA, Hiraku IWAYA,
Kohei TAKIZAWA, Yuriko TANIDA, Takayuki NAITO and Kazuki YANO

Department of Mechanical Systems Engineering, Tokyo University of Agriculture and Technology, Tokyo, Japan

(Received July 28th, 2015)

We have been studying long-lifetime helicon plasma thrusters as the Helicon Electrodeless Advanced Thruster (HEAT) project. Two important elements of the proposed helicon plasma thruster are a generation of a dense source plasma using a helicon wave, and an acceleration of the plasma by the Lorentz force using the product of the induced azimuthal current and static radial magnetic field. Here, in order to eliminate damage of electrodes, both generation and acceleration schemes are operated in non-contact condition between the plasma and electrodes. Acceleration schemes use two type of coils: rotating magnetic field coils and azimuthal mode number $m = 0$ ones. These studies have been carried out on the Large Mirror Device (LMD), which has two types the magnetic field source, permanent magnets and electromagnets, and the Small Helicon Device (SHD), which has small diameter discharge tubes. In this paper, current performances of acceleration schemes are reported.

Key Words: Helicon Plasma Thruster, Electrodeless, Electromagnetic Acceleration

Nomenclature

B	: applied field strength
B_r	: radial component of magnetic field
B_ω	: rotating magnetic field
e	: elementary charge
E_z	: axial component of electric field
F	: thrust
f_{ce}	: electron cyclotron frequency
f_{ci}	: ion cyclotron frequency
$f_{m=0}$: frequency of $m = 0$ coil current
FR	: gas flow rate
f_{RF}	: excitation frequency
f_{RMF}	: frequency of rotating magnetic field
F_z	: axial component of Lorentz force
$I_{m=0}$: current of $m = 0$ coil
I_{RMF}	: current of RMF coil
j_θ	: azimuthal current density
j_z	: axial current density
n_e	: electron density
n_i	: ion density
n_0	: neutral particle density
P	: filling pressure
P_{RF}	: Radio frequency power
r	: radial position
T_e	: electron temperature
$v_{e\theta}$: electron flow velocity
v_i	: ion flow velocity
z	: axial position

1. Introduction

Most practical electric thrusters have a lifetime problem coming from a damage of electrodes directly contacting with a plasma. A helicon plasma thruster is proposed as a long-lifetime electric thruster which has non-direct contact electrodes. This thruster works without any contact electrodes, therefore it has a potential to become a long-lifetime and high-thrust propulsion system, such as a main thruster for a deep space explorer. Development of the helicon plasma thruster has been conducted under the Helicon Electrodeless Advanced Thruster (HEAT) project, in which no electrodes contact with the plasma directly.¹⁾

First, we generate a dense source plasma using a helicon wave with an excitation frequency between an ion and an electron cyclotron frequencies, f_{ci} and f_{ce} , respectively, applied from the outside of a discharge using a radio frequency (RF) antenna. The helicon plasma is known as a high-density ($\sim 10^{19} \text{ m}^{-3}$), a high-ionization ratio (of up to several tens of percent), and a high particle generation efficiency discharge method.²⁾ In addition, its operational ranges are wide and flexible, such as an applied magnetic field B , a fill pressure P and an RF frequency f_{RF} . Second, in order to achieve high thrust and specific impulse, we accelerate the dense plasma source by the axial Lorentz force F_z using the product of the induced azimuthal current j_θ and the static radial magnetic field B_r , shown in Eq. (1).

$$f_z = j_\theta \times B_r \quad (1)$$

There are several methods proposed in our HEAT project for generating j_θ in the high-density source plasma, and our laboratory has been developing schemes that use two types of coils: rotating magnetic field (RMF) coils and an azimuthal mode number $m = 0$ coil.^{1,3-5)} Here, B_r is generated using a combination of permanent magnets, which has relatively large

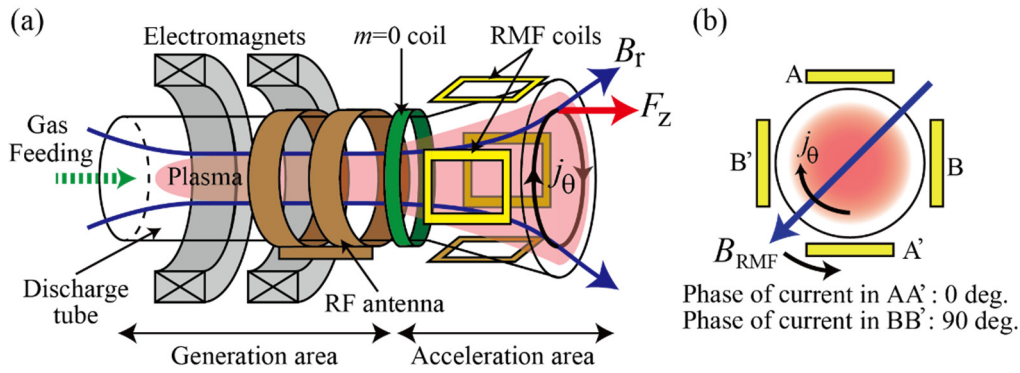


Fig. 1. Schematics of helicon plasma thruster: (a) side view, and (b) cross-sectional view of RMF coils.

B_r component, and electromagnets surrounding a discharge tube to generate the axial field mainly.

To develop these schemes, an estimation of propulsion efficiencies, such as a plasma thrust, a specific impulse and a thrust efficiency, is necessary. In order to measure the thrust, a pendulum-type target stand with a cylindrical target has been developed.⁶⁾ The target type thrust stand is a good solution for measuring the thrust of a large-diameter, complex and heavy system such as our experimental device, Large Mirror Device (LMD).⁷⁾ LMD can accept many diagnostics, such as electrostatic probes (to measure an electron density n_e , an electron temperature T_e , and an ion velocity v_i), spectrometers (gas species, n_e , T_e , and v_i), laser induced fluorescence (v_i and relative n_i), and high-speed camera (plasma plume, relative n_e and n_0). Since various plasma parameters can be derived in this device, we can estimate generation and acceleration schemes in detail.^{1,8,9)}

2. Generation and Acceleration Method

2.1. Generation of the helicon plasma

Figure 1 shows a schematic diagram of the helicon plasma thruster. The magnetic field by permanent magnets and electromagnets (only electromagnets are used in Fig. 1 case) is applied in a generation and an acceleration region. In the generation region, the magnetic field is nearly uniform, but on the other hand, in the acceleration region, there is a strong divergent field (large B_r) having a larger thrust in the presence of j_θ . Inside of a discharge tube, made of a quartz, is filled with a propellant gas (argon and xenon). RF power is fed to the propellant gas via an RF antenna, wound on the outer surface of the discharge tube, thus, the high-density helicon plasma is generated.

2.2. Acceleration: RMF coils method

The RMF scheme was originally developed as a concept to maintain the Field Reversed Configuration (FRC) in a magnetically confined fusion research.³⁾ Here, RMF coils are expected to generate j_θ , as shown in Fig. 1. First, the rotating magnetic field B_ω is generated by two pairs of RMF coils with AC currents, which have a phase difference of 90 degrees between the pairs. Due to the Faraday's law, an axial electric field \widetilde{E}_z is induced. Second, an axial current \widetilde{j}_z is generated by the effects of electron-ion collision and electron-neutral collision through the Ohm's law. Third, the azimuthal electric field is generated by the nonlinear term of $\widetilde{j}_z \cdot \widetilde{B}_r$ (\widetilde{B}_r is radial

AC component of B_ω), and the retarding torque generated by the collision effects again. Azimuthal current j_θ (DC component) is generated as Eq. (2).

$$j_\theta = -n_e e r \cdot 2\pi f_{\text{RMF}} \quad (2)$$

Finally, the axial Lorentz force f_z for plasma acceleration is generated as Eq. (1). Here, j_θ is proportional to n_e and frequency of RMF coil current f_{RMF} , when B_ω is penetrated into the plasma completely.

According to Milroy's theory, our experimental conditions of the RMF acceleration are partial or full penetration.¹⁰⁾ However, we confirmed that the magnetic field was fully penetrated by the use of a magnetic probe.¹¹⁾

2.3. Acceleration: $m = 0$ coil method

$m = 0$ coil is shown in Figure 1(a), located in the acceleration region. In this scheme, the $m = 0$ coil applied with AC current ($f_{m=0} < 100$ kHz) generates an alternating axial magnetic field, which induces alternating j_θ , therefore, this scheme behaves like a transformer. This acceleration method is a half cycle acceleration; the acceleration and deceleration phases. However, the momentum generated in the deceleration phase is canceled due to the collision to the wall of the discharge tube. One of problems is a penetration of the alternating magnetic field into the plasma, same as the RMF scheme. Important operating parameters to achieve the thrust, are the radial component of static magnetic field strength B_r , a frequency of the $m = 0$ coil current $f_{m=0}$, and magneto motive force of $m = 0$ coil.^{1,5)}

3. Experiment

3.1. RMF coils accelerant experiment

Figure 2 shows an experimental setup of LMD. A quartz discharge tube [1,000 mm in length and 100 - 170 mm in inner diameter (i.d.)] has a tapered shape to prevent a wall loss of plasmas in a divergent magnetic field area (acceleration area). This tube is connected to a vacuum chamber (1,700 mm in length and 445 mm in i.d.). LMD has two turbo-molecular pumps (1,000 and 2,400 l/s) with a base pressure $\sim 10^{-4}$ Pa. Argon gas was used as a propellant one, and a typical discharge pressure was > 0.1 Pa. Plasma is generated by a RF power via a half-helical antenna. The RF typical input power P_{RF} and its excitation frequency f_{RF} were ~ 3 kW and 7 MHz, respectively. There were two types of applied magnetic field system;

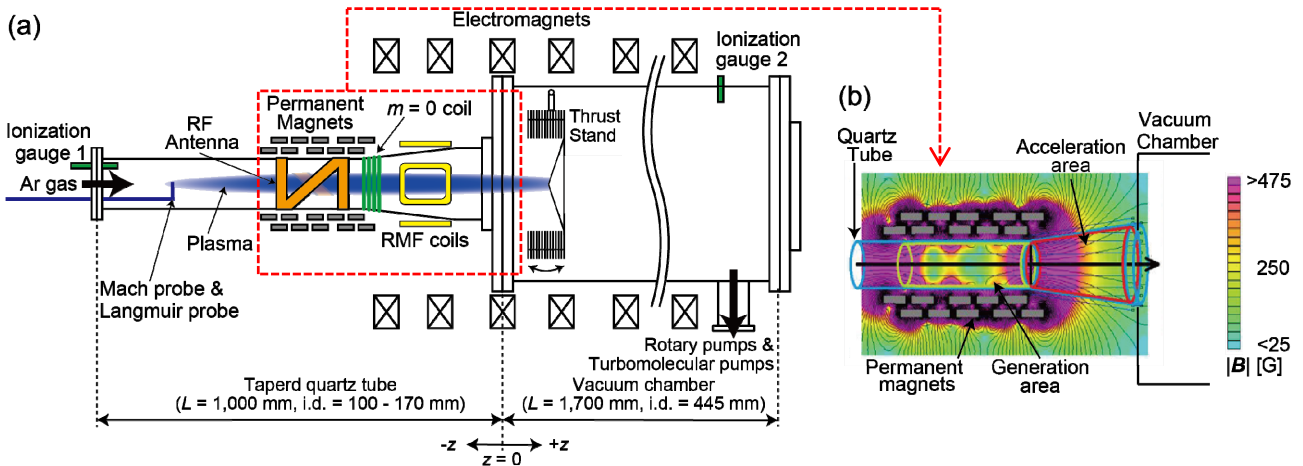


Fig. 2. Experimental set up of LMD: (a) side view of LMD, and (b) expanded view of magnetic field profile generated by permanent magnets.

permanent magnets and electromagnets.¹²⁾ In the case of the RMF experiment, only permanent magnets were used. Permanent magnets placed in the straight section of the quartz tube generate a large radial magnetic field in the acceleration area. Two pairs of RMF coils had 5 turns in each plane (168×115 mm). The material of the RMF coils was oxygen-free copper with 15 mm width and 0.5 mm thickness. The distance between the facing coils was 225 mm, and an axial position of the coil center was $z = -245$ mm, where B_r was large. To check the plasma flow, a Mach probe was used to measure n_e and v_i , employing the unmagnetized model (model constant $\kappa = 1.26$).¹³⁾

Figure 3 indicates v_i and n_e , changing RMF coil current I_{RMF} and gas flow rate FR . In this experiments, P_{RF} and measurement point are 1,000 W and $z = -130$ mm with $r = 60$ mm, respectively. Two types of phase difference between RMF coil current were tested; 90 deg. (acceleration phase) and -90 deg. (deceleration phase). The range of I_{RMF} was 0 - 30 A in the previous research,¹²⁾ which was increased to 50 A in the present experiment. In the cases of acceleration phase, v_i and n_e were increased by increasing I_{RMF} . However, in the cases of deceleration phase, v_i and n_e were almost unchanged. These results indicate that the RMF acceleration scheme is promising. The maximum increasing rates of v_i and n_e were $\sim 19\%$ and $\sim 29\%$, respectively, in the case of $I_{RMF} = 50$ A and $FR = 40$ sccm. As is shown in Fig. 3, the acceleration effect was increased in the case of low gas flow rate, which comes from the low electron-neutral collision frequency.

3.2. $m = 0$ coil acceleration experiment

To verify the $m = 0$ coil acceleration scheme, we have carried out the experiments using the Small Helicon Device (SHD).¹⁴⁻¹⁶⁾ Figure 4(a) shows a side view of this device, which consists of 4 parts, i.e., a gas feeding system, a discharge tube, a vacuum chamber and vacuum pumps. The discharge tube is made of a quartz tube, 20 mm i.d. with an axial length of 453 mm. The vacuum chamber is made of a SUS316 pipe, 165 mm i.d., and 865 mm with an axial length, works as a buffer tank. An electromagnet installed in the discharge tube region generates an axial magnetic field component for generating a source plasma, and a radial component for accelerating the plasma. An RF antenna, installed in an upstream region relative to the

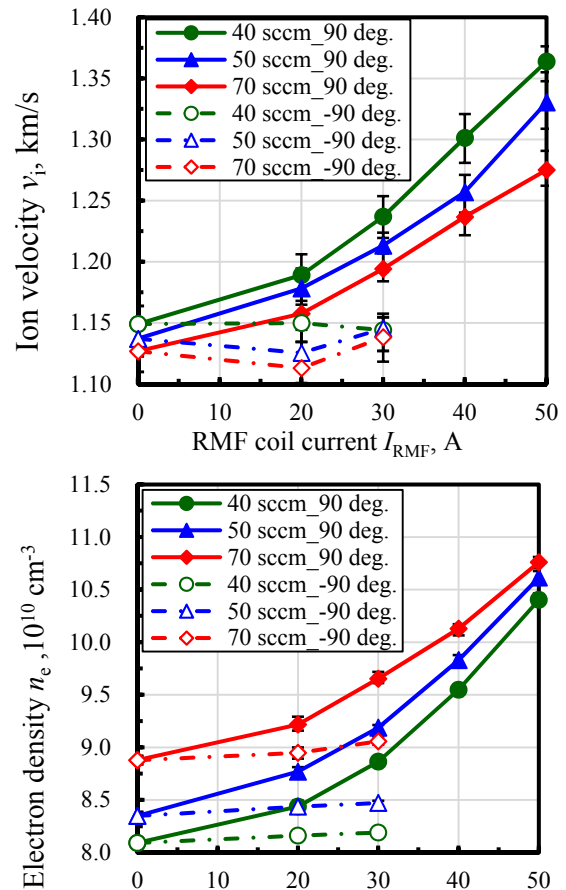


Fig. 3 RMF acceleration effects, i.e., v_i and n_e vs. I_{RMF} and FR ($P_{RF} = 1,000$ W, $z = -130$ mm, and $r = 60$ mm).

electromagnet, transfers RF power up to 2 kW with a frequency of 7 MHz. An $m = 0$ coil is installed in the downstream region of the electromagnet, where the radial field component is large. The detail of the setup in the source region (acceleration region) is indicated in Fig. 4(b).

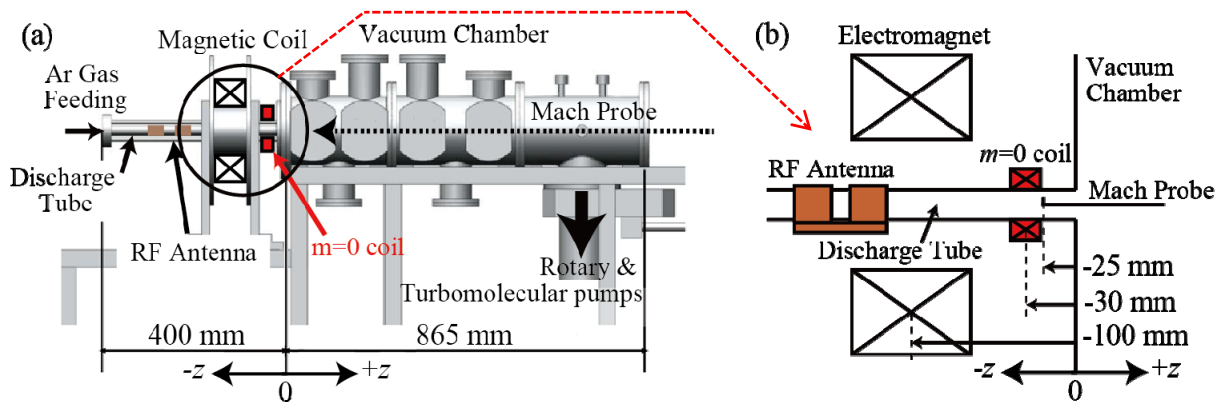


Fig. 4. Experimental set up of SHD: (a) side view of SHD, and (b) expanded view of acceleration region.

Figure 5 shows a preliminary result of the $m = 0$ coil experiment. Red and blue solid lines indicate ion velocities with and without $m = 0$ coil acceleration, respectively. Each ion velocity is measured by the Mach probe at the position of $z = -25$ mm with $r = 0$ and 6 mm. The length of its electrodes is 4 mm in the radial direction. A green dotted line indicates the current of $m = 0$ coil. From the principle, the ion velocity is expected to be accelerated and decelerated alternatively, like the case of $r = 0$ mm. However, in the case of $r = 6$ mm, v_i was accelerating in both accelerating and decelerating phases of $I_{m=0}$, like a wave form of a full wave rectification. In this experiment, a changing of an electron density was small. From these results, we considered that the $m = 0$ coil acceleration was dominant near the central region of the plasma (around $r = 0$), and the Ponderomotive force was also important in the outer edge region of the plasma.¹⁷⁻¹⁹⁾

4. Conclusion

In this paper, the acceleration schemes have been investigated using helicon sources. In order to study the helicon plasma thruster, especially in the plasma acceleration, we have carried out two proposed types of electromagnetic acceleration schemes. The RMF scheme has achieved 19 % increase of v_i . The $m = 0$ coil scheme showed that v_i was increased and decreased alternating in the inner plasma region. On the other hand, v_i was increased in both the acceleration and deceleration phases in the outer plasma region. We considered that these effects in the outer and the center regions were coming from the ponderomotive force and $m = 0$ acceleration, respectively.

Acknowledgement

We appreciate the useful discussion with HEAT project members. This research has been supported partially by Grant-in-Aid for Scientific Research (S: 21226019) from the Japan Society for the Promotion of Science.

References

- 1) Shinohara, S., Nishida, H., Tanikawa, T., Hada, T., Funaki, I. and Shamrai, K. P.: Development of electrodeless plasma thrusters with high-density helicon plasma sources, *IEEE Trans. Plasma Sci.*, **42** (2014), pp. 1245-1254.
- 2) Boswell, R. W.: Plasma production using a standing helicon wave, *Phys. Lett.*, **33A** (1970), pp. 457-458.
- 3) Jones, I. R.: A review of rotating magnetic field current drive and the operation of the rotamak as a field-reversed configuration (Rotamak-FRC) and a spherical tokamak (Rotamak-ST), *Phys. Plasmas*, **6** (1999), pp. 1950-1957.
- 4) Shinohara, S., Hada, T., Motomura, T., Tanaka, K., Tanikawa, T., Toki, K., Tanaka, Y. and Shamrai, K. P.: Development of high-density helicon plasma sources and their applications, *Phys. Plasmas*, **16** (2009), pp. 057104-1-10.
- 5) Ishii, T., Ishii, H., Otsuka, S., Teshigahara, N., Fujitsuka, H., Waseda, S., Kuwahara, D. and Shinohara, S.: Study on electrodeless electric propulsion in high-density helicon plasma with permanent magnets, *JPS Conf. Proc.*, **1** (2014), pp. 015047-1-7.
- 6) Kuwahara, D., Koyama, Y., Otsuka, S., Ishii, T., Ishii, H., Fujitsuka, H., Waseda, S. and Shinohara, S.: Development of direct thrust measurement system for the completely electrodeless helicon plasma thruster, *Plasma Fusion Res.*, **9** (2014), pp. 3406055-1-4.
- 7) Shinohara, S., Takechi, S. and Kawai, Y.: Effects of axial magnetic field and Faraday shield on characteristics of RF produced plasma using spiral antenna, *J. Phys. Soc. Jpn.*, **35** (1996), pp. 4503-4508.

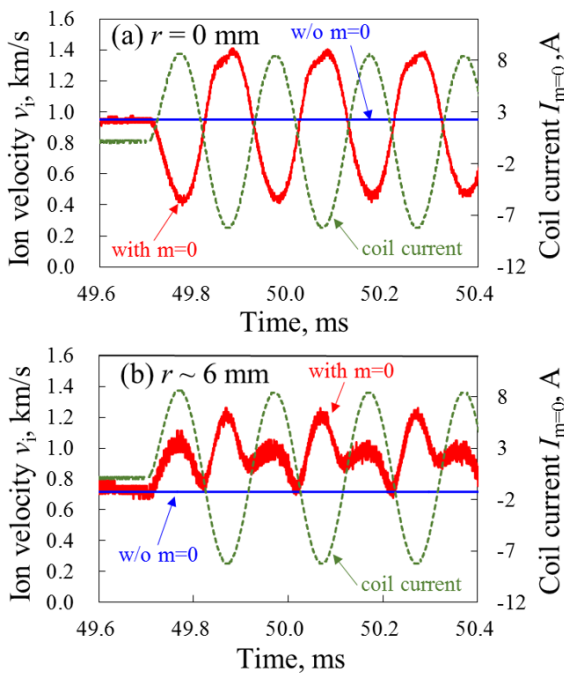


Fig. 5. Experimental results of $m = 0$ coil acceleration: (a) $r = 0$, and (b) $r \sim 6$ mm.

- 8) Teshigahara, N., Shinohara, S., Yamagata, Y., Kuwahara, D. and Watanabe, M.: Development of 2D laser induced fluorescence (LIF) system in high-density helicon plasma, *Plasma Fusion Res.*, **9** (2014), pp. 3406055-1~4.
- 9) Waseda, S., Fujitsuka, H., Shinohara, S., Kuwahara, D., Sakata, M. and Akatsuka, H.: Optical measurements of high-density helicon plasma by using a high-speed camera and monochromators, *Plasma Fusion Res.*, **9** (2014), pp. 3406125-1~4.
- 10) Milroy, R. D.: A numerical study of rotating magnetic fields as a current drive for field reversed configuration, *Phys. Plasmas*, **6** (1999), pp. 2771-2780.
- 11) Otsuka, S., Takizawa, K., Tanida, Y., Kuwahara, D. and Shinohara, S.: Study on plasma acceleration in completely electrodeless electric propulsion system, *Plasma Fusion Res.*, **10** (2015), p. 3401026-1~4.
- 12) Otsuka, S., Nakagawa, T., Ishii, H., Teshigahara, N., Fujitsuka, H., Waseda, S., Ishii, T., Kuwahara, D. and Shinohara, S.: Generation and acceleration of high-density helicon plasma using permanent magnets for the completely electrodeless propulsion system, *Plasma Fusion Res.*, **9** (2014), pp. 3406047-1~5.
- 13) Chung, K. S., Hutchinson, H. H., LaBombard, B. and Conn, R. W.: Plasma flow measurements along the presheath of a magnetized plasma, *Phys. Fluids*, **B1** (1989), p. 2229.
- 14) Kuwahara, D., Mishio, A., Nakagawa, T. and Shinohara, S.: Development of very small-diameter, inductively coupled magnetized plasma device, *Rev. Sci. Instrum.*, **84** (2013), pp. 103502-1~4.
- 15) Nakagawa, T., Shinohara, S., Kuwahara, D., Mishio, A. and Fujitsuka, H.: Characteristics of rf-produced, high-density plasma with very small diameter, *JPS Conf. Proc.*, **1** (2014), pp. 015022-1~5.
- 16) Nakagawa, T., Sato, Y., Tanaka, E., Iwaya, H., Kuwahara, D. and Shinohara, S.: Study on Magnetized RF Discharge with Very Small-Diameter, *Plasma Fusion Res.*, **10** (2015), pp. 3401037-1~4.
- 17) Shinohara, S., Tanikawa, T., Hada, T., Funaki, I., Nishida, H., Matsuoka, T., Otsuka, F., Shamrai, K. P., Rudenko, T. S., Nakamura, T., Mishio, A., Ishii H., Teshigahara, N., Fujitsuka, H. and Waseda, S.: High-density helicon plasma sources: basics and application to electrodeless electric propulsion, *Trans. Fusion Sci. Technol.*, **63** (2014), pp.164-167.
- 18) Otsuka, F., Hada, T., Shinohara, S., Tanikawa, T. and Matsuoka, T.: Numerical studies of Ponderomotive acceleration and ion cyclotron resonance: application to next generation electric thrusters, *Plasma Fusion Res.*, **8** (2013), pp. 2406012-1~14.
- 19) Otsuka, F., Hada, T., Shinohara, S., Tanikawa, T. and Matsuoka, T.: Numerical modeling of electrodeless electric thruster by ion cyclotron resonance/Ponderomotive acceleration, *Plasma Fusion Res.*, **8** (2013), pp. 2406067-1~7.